



Crossband versus intraband pairing in superconductors: Signatures and consequences of the interplay

A. A. Vargas-Paredes,^{1,2} A. A. Shanenko³,,³ A. Vagov,⁴ M. V. Milošević,^{2,*} and A. Perali¹

¹*School of Pharmacy, Physics Unit, Università di Camerino, I-62032 Camerino, Italy*

²*Department of Physics, University of Antwerp, Groenenborgerlaan 171, B-2020 Antwerp, Belgium*

³*Universidade Federal de Pernambuco, Avenida Professor Luiz Freire, s/n, 50670-901 Recife-PE, Brazil*

⁴*Institut für Theoretische Physik III, Bayreuth Universität, D-95440 Bayreuth, Germany*



(Received 18 June 2019; revised manuscript received 8 March 2020; accepted 9 March 2020; published 27 March 2020)

We analyze the paradigmatic competition between intraband and crossband Cooper-pair formation in two-band superconductors, neglected in most works to date. We derive the phase-sensitive gap equations and describe the crossover between the intraband-dominated and the crossband-dominated regimes, delimited by a “gapless” state. Experimental signatures of crosspairing comprise notable gap splitting in the excitation spectrum, non-BCS behavior of gaps versus temperature, as well as changes in the pairing symmetry as a function of temperature. The consequences of these findings are illustrated on the examples of MgB_2 and $\text{Ba}_{0.6}\text{K}_{0.4}\text{Fe}_2\text{As}_2$.

DOI: [10.1103/PhysRevB.101.094516](https://doi.org/10.1103/PhysRevB.101.094516)

I. INTRODUCTION

Multiband superconductivity is known to promote novel quantum phenomena of great fundamental importance and versatility [1]. Among recent examples are optically excited collective modes in multiband MgB_2 [2], the emergent phenomena at the BCS-BEC crossover in FeSe [3], and at oxide interfaces [4]. The strong scientific appeal of multiband superconductivity stems from its pronounced tunability. External pressure, lattice strain effects, gating, chemical doping, photoinduction, quantum confinement, and surface effects are all able to move and change the band dispersions and the position of the chemical potential with respect to Lifshitz transitions [4–9], where superconducting properties can radically change.

To date, the multiband electronic structure has proven to be of crucial importance in rather versatile superconducting systems, such as MgB_2 [10], iron-based compounds [11–16], superconducting nanostructures [17–21], two-dimensional (2D) electron gases at interfaces [22–24], metal-organic superconductors [25–27], etc. In such multiband superconductors, the pairing interaction and the proximity/hybridization of two or more bands can result in the formation of Cooper pairs with electrons originating from different bands, a phenomenon termed “crossband pairing” or simply “crosspairing.” Particularly, the proximity of the bands allows one to justify the Cooper instability driven by an attractive interaction with a sizable enough energy scale as the mechanism behind crosspairing. Moreover, in the case that the pairing interaction strongly depends on the momentum, then one is able to connect different Fermi-surface pockets [28], which promotes crosspairing. This pairing is to be distinguished from the Josephson-like pair transfer between intraband condensates,

which is usually taken as their sole coupling in multiband superconductors. Crosspairing and intraband pairing are intuitively competitive, therefore it is necessary to understand their interplay qualitatively and quantitatively, together with associated changes in physical properties and observables. Such an understanding is far from established, as crosspairing in competition with intraband pairing has been predominantly neglected in studies to date. In superfluid systems with at least two fermionic species, the partially overlapping bands at the Fermi level are prone to crosspairing, as discussed in Refs. [29,30]. In superconductors, the hybridization of multiple bands close to the Fermi level is favorable for crossband pair formation. This occurs in the iron-based superconductors (FeSCs) which present hybridized orbitals [31,32], cuprates with the hybridization of $d_{x^2-y^2}$ and d_{z^2} orbitals [33,34], and also in the heavy-fermion compounds, where crosspairing between electrons with f and d orbital character has been considered [35]. However, even without hybridization, the plain proximity of multiple bands can facilitate crosspairing, as illustrated in Fig. 1 for bulk and atomically thin MgB_2 or field-effect doping in strained MoS_2 nanolayers [36].

In this paper, we examine the interplay between intra- and crossband pairing in two-band superconductors and its experimental signatures. The paper is organized as follows. In Sec. II we present our theoretical model. Section III contains the obtained results, starting from the startling behavior of the excitation gaps in the presence of crosspairing and the discussion of a possible “gapless” state. Further discussion comprises the quantification of the reported effects in cases of some exemplified multiband (and multigap) materials, and possible emergent phase-dependent (phase-frustrated) phenomena as a function of temperature. Our findings are summarized in Sec. IV, where an outlook to possible further studies is also given.

*milorad.milosevic@uantwerpen.be

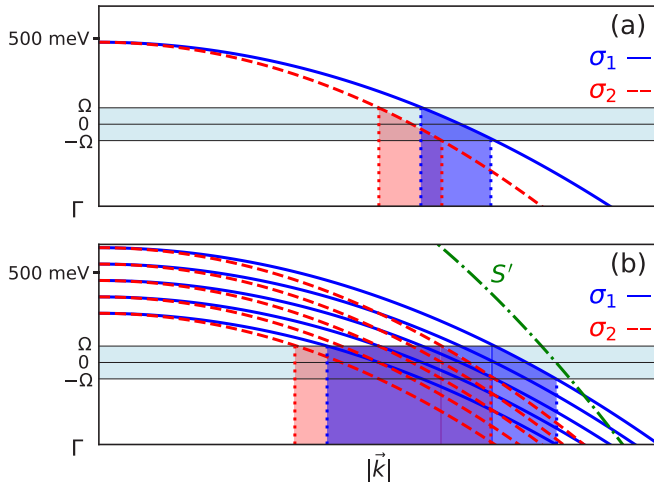


FIG. 1. The relevance of crosspairing is illustrated based on the band structure of (a) bulk MgB₂ [37] and (b) 6-monolayer MgB₂ [38]. Only σ bands close to the Γ point of the Brillouin zone are shown, with chemical potential $\mu = 500$ meV and energy scale of the pairing $\Omega = 75$ meV. In (b), each interior monolayer contributes a pair of holelike bands σ_1 and σ_2 , and the surface band is denoted by S' . The (purple) overlapping shadows project the momentum states where crossband pairing between opposite momenta states among the σ bands is feasible.

II. THEORETICAL FORMALISM

We reformulate the mean-field equations for the superconducting order parameter, going beyond the Suhl, Matthias, and Walker (SMW) extension of the BCS theory [39]. This results in an extended self-consistent and phase-dependent set of equations for the several components of the order parameter, with strongly hybridized excitation spectra. The mean-field Hamiltonian including both intraband and crossband pairing reads

$$H = \sum_{i,\mathbf{k},\sigma} \epsilon_i(\mathbf{k}) c_{i,\mathbf{k}\sigma}^\dagger c_{i,\mathbf{k}\sigma} + H_{\text{int}}, \quad (1)$$

$$H_{\text{int}} = \sum_{i,j} \sum_{\mathbf{k}} [\Delta_{ij}(\mathbf{k}) c_{i,\mathbf{k}\uparrow}^\dagger c_{j,-\mathbf{k}\downarrow}^\dagger + \text{H.c.}], \quad (2)$$

where $i, j = 1, 2$ represent the band index, and $\sigma = \uparrow, \downarrow$ the spin. Here, $\Delta_{ij}(\mathbf{k}) = \sum_{k,l=1,2} \sum_{\mathbf{k}'} V_{ij,kl}(\mathbf{k}, \mathbf{k}') \langle c_{k,-\mathbf{k}'\uparrow} c_{l,\mathbf{k}'\downarrow} \rangle$ are the pairing amplitudes, and $\epsilon_i(\mathbf{k})$ is the band-dependent kinetic energy of the electrons. We note that Eq. (1) resembles the Hamiltonian of a two-band system with hybridization upon the change from orbital to the band basis [32]. The full \mathbf{k} -dependent form of the interaction matrix is given by $V_{ij,kl}(\mathbf{k}, \mathbf{k}') = -g_{ij,kl} \Theta(\Omega - |\zeta_i(\mathbf{k})|) \Theta(\Omega - |\zeta_j(\mathbf{k}')|) \Theta(\Omega - |\zeta_k(\mathbf{k}')|) \Theta(\Omega - |\zeta_l(\mathbf{k})|)$, where Ω is the average energy scale of the effective interaction, and $\zeta_i(\mathbf{k}) = \epsilon_i(\mathbf{k}) - \mu$ with chemical potential μ . In $g_{ij,kl} =$

$$\begin{pmatrix} g_{11,11} & g_{11,22} & g_{11,(12)} \\ g_{22,11} & g_{22,22} & g_{22,(12)} \\ g_{(12),11} & g_{(12),22} & g_{(12),(12)} \end{pmatrix},$$

the upper left 2×2 inner matrix corresponds to the well-established SMW case [39], and the third row and column include the crosspairing [where (12) indicates symmetrization under given indices, so that, e.g., $g_{(12),(12)} = g_{12,12} + g_{21,21}$]. In the interaction matrix the effective attraction between electrons is given by its diagonal

elements, and the off-diagonal ones describe the Josephson-like coupling between intraband and crossband condensates.

In what follows, we simplify our indices as $11 \equiv 1, 22 \equiv 2$, and $(12) \equiv 3$. Next, we use the Gor'kov Green's function formalism to obtain the pair amplitude equations [19,40]. In momentum space the two excitation spectra without crosspairing ($i = 1, 2$) are $\epsilon_i^2 = \zeta_i^2 + |\Delta_i|^2$ and the pair amplitudes are given by $\Delta_i(\mathbf{k}) = |\Delta_i| e^{i\varphi_i} \Theta(\Omega - |\zeta_i(\mathbf{k})|)$, where φ_i is the phase of the pair amplitude.

The crosspairing pair amplitude Δ_3 hybridizes the energy spectra of the two BCS-like excitation branches,

$$E_{\pm}(\theta) = \sqrt{\frac{1}{2} [\epsilon_1^2 + \epsilon_2^2 + 2|\Delta_3|^2 \pm b(\theta)]}, \quad (3)$$

$$b(\theta) = \sqrt{(\epsilon_1^2 - \epsilon_2^2)^2 + 4|\Delta_3|^2 r(\theta)}, \quad (4)$$

where $r = (\zeta_1 - \zeta_2)^2 + |\Delta_1|^2 + |\Delta_2|^2 + 2|\Delta_1||\Delta_2| \cos \theta$ and $\theta = 2\varphi_3 - \varphi_1 - \varphi_2$. We emphasize here that the angle θ will introduce other degrees of freedom in our system depending on the combination of the couplings, as will be shown later. The excitation gaps $\Delta_{\pm}(\theta)$ coincide with the minimum energy of the excitation branches $E_{\pm}(\theta)$. These are the two gaps Δ_{\pm} present in the density of states (DOS), however, these gaps no longer correspond to the energy needed to break intraband Cooper pairs (as is conventionally the case). Instead, they describe the energy needed to disallow *either* intra- or crossband pairing.

The self-consistent equations for the pair amplitudes are given by

$$\Delta_i = \frac{1}{2} \sum_j g_{ij} \int \frac{d^3k}{(2\pi)^3} \Delta_j [\chi_j^+ f(E_+) + \chi_j^- f(E_-)], \quad (5)$$

where $f(E) = \frac{1}{2E} \tanh(\frac{\beta E}{2})$, $\chi_i^{\pm} = 1 \pm \frac{1}{b(\theta)} \chi_i$, $\chi_{1(2)} = \epsilon_{1(2)}^2 - \epsilon_{2(1)}^2 + 2|\Delta_3|^2(1 + |\Delta_{2(1)}|e^{i\theta}/|\Delta_{1(2)}|)$, $\chi_3 = (\zeta_1 - \zeta_2)^2 + |\Delta_1|^2 + |\Delta_2|^2 + 2|\Delta_1||\Delta_2|e^{-i\theta}$, and $\beta = 1/k_B T$. Note that these pairing amplitudes (i.e., the order parameters in the problem) *do not correspond* to the experimentally measurable gaps Δ_{\pm} .

III. RESULTS AND DISCUSSION

Before solving the above formalism to reveal the different physics brought by crosspairing, we introduce parabolic bands and dimensionless effective couplings, $\lambda_{ij} = g_{ij} N_j(0)$, where $N_{j=1,2}(0)$ is the band-dependent density of states and $N_3(0) = N_1(0) + N_2(0)$. We start by solving Eq. (5) when all couplings λ_{ij} are positive and with the same phase, i.e., $\theta = 0$. To visualize the effect of crosspairing we fix all parameters but λ_{33} : $E_F = 200$ meV, $\Omega = 30$ meV, $\lambda_{11} = 0.4$, $\lambda_{22} = 0.3$, $\lambda_{ij,i \neq j} = 0.05$.

A. Excitation gaps in the presence of crosspairing

In Figs. 2(a) and 2(b), we show the excitation gaps and all three pairing amplitudes at 4.2 K. As crosspairing coupling λ_{33} is increased, the two excitation gaps Δ_+ and Δ_- are split further apart: Increasing Δ_3 strengthens Δ_+ and suppresses Δ_- . In other words, Δ_3 interacts constructively with Δ_1 and destructively with Δ_2 , generating Δ_+ and Δ_- , respectively.

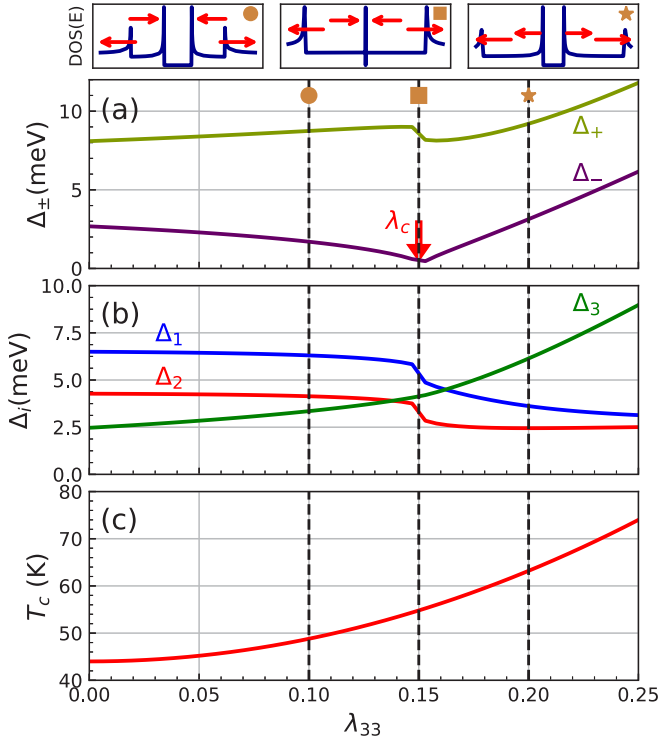


FIG. 2. Effect of crosspairing for the same phase. (a) Excitation gaps with their (b) corresponding pair amplitudes as a function of λ_{33} at $T = 4.2$ K. The three miniplots above (a) show the density of states for $\lambda_{33} = 0.1, 0.15,$ and 0.2 , illustrating the behavior in the intraband-dominated regime, gapless state, and the crosspairing dominated regime, respectively. (c) Mean-field critical temperature vs λ_{33} .

This occurs up to a characteristic value $\lambda_{33} = \lambda_c$ (roughly half the average of λ_{11} and λ_{22}). This characteristic value marks the maximal competition between the intraband and the crossband pairing channels and separates the two regimes: the intraband-dominated regime (IDR) for $\lambda_{33} < \lambda_c$, and a crosspairing-dominated regime (CDR) for $\lambda_{33} > \lambda_c$. In the CDR, both gaps increase at the same rate, similarly to the one-band scenario. Therefore the CDR describes a two-gap system which is characterized by a sole order parameter Δ_3 , while the intraband pair amplitudes participate only passively, by proximity [41,42]. Figure 2(c) shows that superconducting critical temperature T_c increases with λ_{33} faster than expected considering the range of values of λ_{33} alone.

In the miniplots above Fig. 2(a), we show the density of states [as a measurable quantity in scanning tunneling microscopy (STM)/scanning tunneling spectroscopy (STS)] for the IDR, CDR, as well as for the crossover point $\lambda_{33} = \lambda_c$. Note that in the latter situation the inner coherence peak approaches zero energy, and may disappear at exactly zero for a favorable combination of parameters. That case would mark a *gapless regime*, where the weaker gap is no longer directly detectable, but all contributing pair amplitudes still play a role in all observables in, e.g., applied magnetic field or transport measurements. Note that this situation is very different from the gapless state in a two-band superconductor at the symmetry-breaking transition due to impurity scattering

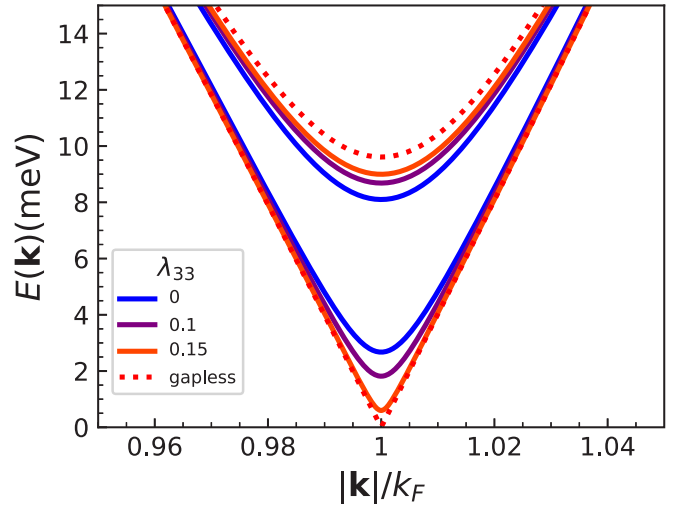


FIG. 3. Energy dispersions corresponding to Fig. 2, for λ_{33} increased towards the gapless state.

[43,44]. In the present case, we consider a clean system where superconducting gaps extracted from the tunneling spectra of STM would no longer coincide with the ones extracted from low-temperature angle-resolved photoemission spectroscopy (ARPES) [45] using a normal-state band structure as a reference. Moreover, the lowest-energy excitation branch exhibits a linear V-shaped dispersion in our gapless state (see Fig. 3). Such a multiband system has a peculiar multicomponent composition, with the coexistence of a large-gap condensate and the in-gap states having a free-particle character. This leads to a finite DOS at low energies (without any disorder present), and a radically changed temperature dependence of all superconducting properties with respect to the gapped state. These emergent properties make the gapless state induced by crosspairing a unique feature of multiband superconductors, worthy of further investigation.

B. Example of MgB₂

To quantify the effects of crosspairing, it is instructive to take the example of the best-known two-gap superconductor MgB₂ [46]. This superconductor has four contributing bands, two σ bands for the stronger gap and two π bands for the weaker one. The distance of two σ bands in the vicinity of the Fermi level is approximately 75 meV [see Fig. 1(a)]. Taking the parameters $\mu = 500$ meV and $\Omega = 75$ meV from Refs. [37,47], we consider the crosspairing between the σ bands, with the coupling matrix

$$\lambda_{ij} = \begin{pmatrix} 0.275 & 0.032 & \lambda_{i3} & 0.032 \\ 0.032 & 0.274 & \lambda_{i3} & 0.032 \\ \lambda_{i3} & \lambda_{i3} & 0.1 & 0.01 \\ 0.01 & 0.01 & 0.01 & 0.22 \end{pmatrix}. \quad (6)$$

The above matrix is asymmetric because of different DOS associated with each band. λ_{i4} is the coupling to the π bands, and the third column and row correspond to the coupling to the crosspairing channel, with λ_{i3} as a free (small) parameter. Other coupling constants are taken from the literature, and yield the experimentally verified gaps of MgB₂ (≈ 7 and

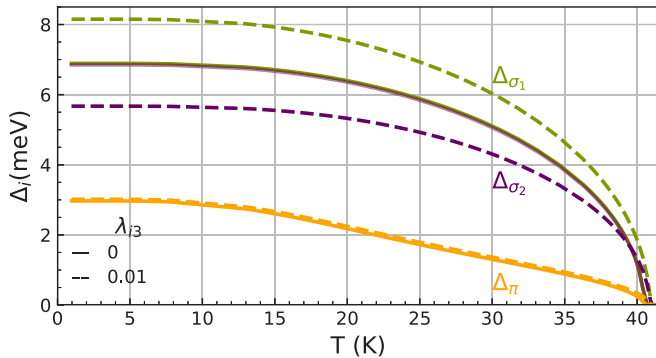


FIG. 4. Superconducting gaps of bulk MgB_2 as a function of temperature, for intraband pairing only (solid lines), and in the presence of weak crosspairing (dashed lines).

3 meV) in the absence of crosspairing ($\lambda_{i3} = 0$, see Fig. 4). Even a small $\lambda_{i3} = 0.01$ yields a 2 meV split of the two σ gaps and a 1 K increase in T_c . This gives confidence that crosspairing effects, even if seemingly small, can lead to significant modifications of the gap spectrum without significantly changing T_c . That in turn calls for the revisiting of theoretical approaches, e.g., to include crosspairing in anisotropic Eliashberg calculations even for materials that seemed previously well described [48,49], as well as revisiting the available experimental data (bearing in mind the nonequivalence between Δ_{\pm} and the pairing amplitudes in the presence of crosspairing). Conducting more refined ARPES measurements (e.g., in the case of crystalline MgB_2 , on two σ bands separately) can provide evidence for the gap splitting caused by crosspairing.

C. Phase-frustrated phenomena

Last but not least, we discuss the phase-frustrated solutions of Eq. (5), with nonzero angle θ . For example, in the family of FeSCs one can have two cases where a nontrivial phase difference is present. The first is the conventional s_{\pm} case, which contemplates a π -phase difference between electronlike and holelike pair amplitudes [50]. The second is the orbital antiphase s_{\pm} case, with a π -phase difference between bands of the same type (electronlike or holelike), as reported in the optimally doped $(\text{BaK})\text{Fe}_2\text{As}_2$ ($T_c = 36$ K) [51–53]. This compound presents two holelike bands (α, β) stemming from two nested Fermi sheets at the Γ point, and two electronlike bands (γ, δ) stemming from two nested Fermi sheets at the M point. The proximity of both pairs of bands to the Fermi level and the smallness of their interband distance justifies the assumption of crosspairing between bands α and β or γ and δ . To identify the emergent effects, we will consider the effect of crosspairing only between α and β (assuming similar consequences for crosspairing between γ and δ). We take the interband distance between α and β as 10 meV and the Fermi level at $\mu = 50$ meV, following Ref. [54]. To obtain the gaps (Δ_{\pm}) as measured in the low-temperature experiments of Ref. [16] (≈ 12.4 and 6.2 meV extrapolated to $T = 0$), we take

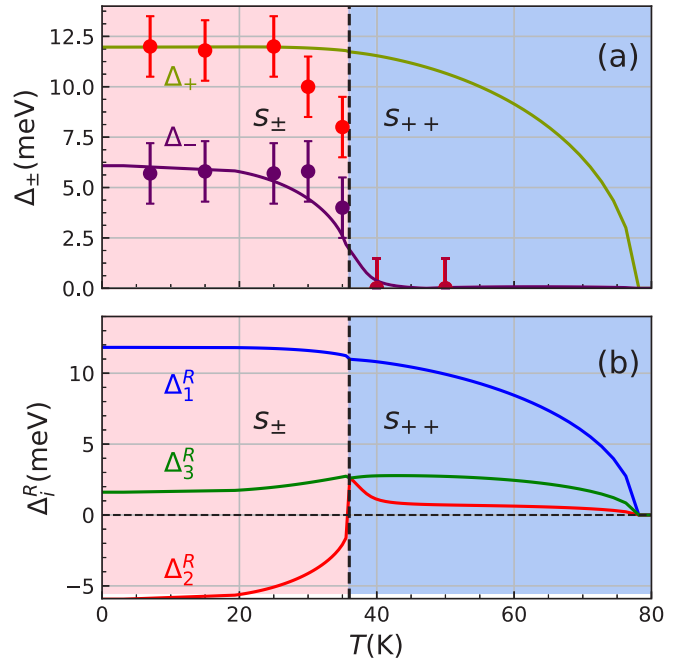


FIG. 5. (a) Excitation gaps Δ_{\pm} , and (b) real part of the pair amplitudes Δ_i^R as a function of temperature, for parameters of (α, β) bands in $(\text{BaK})\text{Fe}_2\text{As}_2$, with nominal s_{\pm} antiphase and in the presence of crosspairing. Data points with error bars are the experimentally measured gaps of $\text{Ba}_{0.6}\text{K}_{0.4}\text{Fe}_2\text{As}_2$ [16]. For microscopic parameters reproducing the experimentally measured gaps at zero temperature (see text), an $s_{\pm} \rightarrow s_{++}$ transition is found at 36 K, corresponding to the critical temperature of the measured gaps at the Γ point of $\text{Ba}_{0.6}\text{K}_{0.4}\text{Fe}_2\text{As}_2$ [16].

for the coupling matrix

$$\lambda_{ij} = \begin{pmatrix} 0.51 & \lambda_{12} & \lambda_{13} \\ 0.5\lambda_{12} & 0.39 & \lambda_{13} \\ 0.5\lambda_{13} & 0.5\lambda_{13} & 0.25 \end{pmatrix}. \quad (7)$$

Here, λ_{12} is taken negative, which is the standard way to obtain the sign change in the band-dependent order parameters (as reported in $\text{Ba}_{0.6}\text{K}_{0.4}\text{Fe}_2\text{As}_2$ [55]). We introduce a weak repulsion $\lambda_{12} = -0.005$, which induces a phase shift between the two intraband pair amplitudes, $\varphi_1 - \varphi_2 = \pi$. In such a case, the coupling of the crosspairing pair amplitude with the intraband pair amplitudes (for $\lambda_{i3} > 0$) will introduce frustration on the phase of the crosspairing order parameter φ_3 . Phase frustration of a similar sort is known in three-band systems [56–58] and can lead to skyrmionic vortex states [59–61], but is not possible in a two-band system unless crosspairing is present. In the present case, we reveal additional different physics, as crosspairing induces an $s_{\pm} \rightarrow s_{++}$ transition as a function of temperature, as shown in Figs. 5(a) and 5(b) for exemplified parameters of $(\text{BaK})\text{Fe}_2\text{As}_2$. Here, it is important to differentiate our results from the $s_{\pm} \rightarrow s_{++}$ transition found earlier due to impurities [62] or due to symmetry breaking at the sample surface of a two-band s_{\pm} superconductor [63]. The transition reported here is solely caused by crosspairing, and presents an entirely different aspect in the analysis of time-reversal symmetry breaking in multiband superconductors.

In the example shown in Figs. 5(a) and 5(b) based on (BaK)Fe₂As₂, after the $s_{\pm} \rightarrow s_{++}$ transition, the pair amplitudes recover the same phase ($\theta = 0$) up to the expected BCS critical temperature of ≈ 80 K. However, in the experiment of Ref. [16], the superconducting gaps abruptly cease at $T_c \approx 40$ K, for reasons not understood to date. Without claiming to describe the experimentally observed non-BCS temperature behavior of the gaps, we notice that our gaps Δ_+ and Δ_- in Fig. 5(a) very closely match the experimentally measured ones up to the experimentally observed T_c of 36 K, and the temperature of the crosspairing-driven $s_{\pm} \rightarrow s_{++}$ transition exactly matches the experimentally observed T_c where superconductivity abruptly ceases. In other words, an s_{\pm} two-band system, with substantial crosspairing present, can exhibit a non-BCS-like temperature dependence of the gaps in cases when the transition from the s_{\pm} to the s_{++} order is disallowed in any way.

IV. CONCLUSIONS AND OUTLOOK

In summary, although mostly neglected to date, the crossband pairing in multiband superconductors is certainly of importance in materials with hybridized or energetically close bands in the vicinity of the Fermi level. In this regime, the interplay between intra- and crossband pairing leads to several unique effects. For one, crossband pairing increases the splitting between intraband gaps, with a tendency to decrease the weaker gap towards an entirely different “gapless” state, signatures of which will still be observable since a vanishing gap does not imply vanishing order parameter(s) in this regime. The crosspairing also introduces the possibility of a phase frustration between the pairing channels, leading to other transitions as a function of temperature (such as $s_{\pm} \rightarrow s_{+++}$), and a likely nontrivial response of the superconductor to, e.g., the magnetic field [64]. Our results call for revisiting the existing theories and experimental data for multiband superconductors with close bands, bearing in mind

also that the band dispersions and chemical potential can be tuned towards a parameter regime where the above-mentioned signatures of crosspairing can be detected. In that context, we point out the most recent measurements of Ref. [4], where the tunability of multiple gaps has been achieved at the oxides’ interface by gate doping around a Lifshitz transition, as the closest experimental system to our present model.

Besides the needed generalization to the case of multiple (3+) bands, the outlook of the present study is very broad. It includes understanding the effects of impurities, particularly magnetic ones where DOS signatures of crosspairing near a gapless state can overlap with the Majorana zero-energy bound state [65,66]. It is also of interest to further examine the intra- to crosspairing competition in the presence of spin-flip scattering [67], oddness in parity [15], and photoinduced phenomena [9,68]. Even beyond superconductivity, crosspairing and its competition with intraband pairing remains insufficiently explored in molecular optics [69], multicomponent superfluidity [29], and quantum chromodynamics [30].

ACKNOWLEDGMENTS

This collaborative work was fostered within the international MultiSuper network on Multi-condensate Superconductivity and Superfluidity [70]. The authors thank Andrea Guidini for his help during the initial stage of this work and Laura Fanfarillo for useful discussions. This work was partially supported by the Italian MIUR through the PRIN 2015 program (Contract No. 2015C5SEJJ001) and the Research Foundation - Flanders (FWO). A.A.V.-P. acknowledges support by the joint doctoral program and by the Erasmus+ exchange between the University of Antwerp and the University of Camerino. M.V.M. gratefully acknowledges support from a Visiting Professorship at the University of Camerino. A.S. and A.V. acknowledge support from the CAPES/Print Grant, Process No. 88887.333666/2019-00 (Brazil) and the Russian Science Foundation Project No. 18-12-00429, respectively.

-
- [1] M. V. Milošević and A. Perali, Emergent phenomena in multicomponent superconductivity: An introduction to the focus issue, *Supercond. Sci. Technol.* **28**, 060201 (2015).
 - [2] F. Giorgianni, T. Cea, C. Vicario, C. P. Hauri, W. K. Withanage, X. Xi, and L. Benfatto, Leggett mode controlled by light pulses, *Nat. Phys.* **15**, 341 (2019).
 - [3] T. Hanaguri, S. Kasahara, J. Böker, I. Eremin, T. Shibauchi, and Y. Matsuda, Quantum Vortex Core and Missing Pseudogap in the Multiband BCS-BEC Crossover Superconductor FeSe, *Phys. Rev. Lett.* **122**, 077001 (2019).
 - [4] G. Singh, A. Jouan, G. Herranz, M. Scigaj, F. Sánchez, L. Benfatto, S. Caprara, M. Grilli, G. Saiz, F. Couëdo, C. Feuillet-Palma, J. Lesueur, and N. Bergeal, Gap suppression at a Lifshitz transition in a multi-condensate superconductor, *Nat. Mater.* **18**, 948 (2019).
 - [5] Y. Li, C. An, C. Hua, X. Chen, Y. Zhou, Y. Zhou, R. Zhang, C. Park, Z. Wang, Y. Lu, Y. Zheng, Z. Yang, and Z. Xu, Pressure-induced superconductivity in topological semimetal NbAs₂, *npj Quantum Mater.* **3**, 58 (2018).
 - [6] W.X. Li, R. Zeng, L. Lu, and S.X. Dou, Dependence of superconducting properties on lattice strain in MgB₂, *Physica C* **470**, S629 (2010).
 - [7] D. Costanzo, S. Jo, H. Berger, and A. F. Morpurgo, Gate-induced superconductivity in atomically thin MoS₂ crystals, *Nat. Nanotechnol.* **11**, 339 (2016).
 - [8] A. Continenza and G. Profeta, Chemical doping in pnictides superconductors: The case of Ca(Fe_{1-x}X_x)₂As₂, X = Co, Ni, Pt, *J. Magn. Magn. Mater.* **452**, 179 (2018).
 - [9] S. Porta, L. Privitera, N. Traverso Ziani, M. Sasseti, F. Cavaliere, and B. Trauzettel, Feasible model for photoinduced interband pairing, *Phys. Rev. B* **100**, 024513 (2019).
 - [10] J. Nagamatsu, N. Nagakawa, T. Muranaka, Y. Zenitani, and J. Akimitsu, Superconductivity at 39 K in magnesium diboride, *Nature (London)* **410**, 63 (2001).
 - [11] L. de’ Medici, G. Giovannetti, and M. Capone, Selective Mott Physics as a Key to Iron Superconductors, *Phys. Rev. Lett.* **112**, 177001 (2014).

- [12] L. Benfatto, B. Valenzuela, and L. Fanfarillo, Nematic pairing from orbital-selective spin fluctuations in FeSe, *npj Quantum Mater.* **3**, 56 (2018).
- [13] R. Yu, J.-X. Zhu, and Q. Si, Orbital Selectivity Enhanced by Nematic Order in FeSe, *Phys. Rev. Lett.* **121**, 227003 (2018).
- [14] J. Herbrych, N. Kaushal, A. Nocera, G. Alvarez, A. Moreo, and E. Dagotto, Spin dynamics of the block orbital-selective Mott phase, *Nat. Commun.* **9**, 3736 (2018).
- [15] A. M. Black-Schaffer and A. V. Balatsky, Odd-frequency superconducting pairing in multiband superconductors, *Phys. Rev. B* **88**, 104514 (2013).
- [16] H. Ding, P. Richard, K. Nakayama, K. Sugawara, T. Arakane, Y. Sekiba, A. Takayama, S. Souma, T. Sato, T. Takahashi, Z. Wang, X. Dai, Z. Fang, G. F. Chen, J. L. Luo, and N. L. Wang, Observation of Fermi-surface-dependent nodeless superconducting gaps in $\text{Ba}_{0.6}\text{K}_{0.4}\text{Fe}_2\text{As}_2$, *Europhys. Lett.* **83**, 47001 (2008).
- [17] A. Bianconi, A. Valletta, A. Perali, and N. L. Saini, High T_c superconductivity in a superlattice of quantum stripes, *Solid State Commun.* **102**, 369 (1997).
- [18] A. Valletta, A. Bianconi, A. Perali, and N. L. Saini, Electronic and superconducting properties of a superlattice of quantum stripes at the atomic limit, *Z. Phys. B: Condens. Matter* **104**, 707 (1997).
- [19] A. A. Shanenko, J. Albino Aguiar, A. Vagov, M. D. Croitoru, and M. V. Milošević, Atomically flat superconducting nanofilms: Multiband properties and mean-field theory, *Supercond. Sci. Technol.* **28**, 054001 (2015).
- [20] L. Flammia, L.-F. Zhang, L. Covaci, A. Perali, and M. V. Milošević, Superconducting nanoribbon with a constriction: A quantum-confined Josephson junction, *Phys. Rev. B* **97**, 134514 (2018).
- [21] L.-F. Zhang, L. Flammia, L. Covaci, A. Perali, and M. V. Milošević, Multifaceted impact of a surface step on superconductivity in atomically thin films, *Phys. Rev. B* **96**, 104509 (2017).
- [22] D. Valentinis, S. Gariglio, A. Fête, J.-M. Triscone, C. Berthod, and D. van der Marel, Modulation of the superconducting critical temperature due to quantum confinement at the $\text{LaAlO}_3/\text{SrTiO}_3$ interface, *Phys. Rev. B* **96**, 094518 (2017).
- [23] N. Mohanta and A. Taraphder, Multiband theory of superconductivity at the $\text{LaAlO}_3/\text{SrTiO}_3$ interface, *Phys. Rev. B* **92**, 174531 (2015).
- [24] T. V. Trevisan, M. Schütt, and R. M. Fernandes, Unconventional Multiband Superconductivity in Bulk SrTiO_3 and $\text{LaAlO}_3/\text{SrTiO}_3$ Interfaces, *Phys. Rev. Lett.* **121**, 127002 (2018).
- [25] R.-S. Wang, Y. Gao, Z.-B. Huang, and X.-J. Chen, Superconductivity above 120 kelvin in a chain link molecule, [arXiv:1703.06641](https://arxiv.org/abs/1703.06641).
- [26] X. Zhang, Y. Zhou, B. Cui, M. Zhao, and F. Liu, Theoretical discovery of a superconducting two-dimensional metal-organic framework, *Nano Lett.* **17**, 6166 (2017).
- [27] M. V. Mazziotti, A. Valletta, G. Campi, D. Innocenti, A. Perali, and A. Bianconi, Possible Fano resonance for high- T_c multi-gap superconductivity in p-terphenyl doped by K at the Lifshitz transition, *Europhys. Lett.* **118**, 37003 (2017).
- [28] A. Perali, C. Castellani, C. Di Castro, M. Grilli, E. Piegari, and A. A. Varlamov, Two-gap model for underdoped cuprate superconductors, *Phys. Rev. B* **62**, R9295 (2000).
- [29] W. V. Liu and F. Wilczek, Interior Gap Superfluidity, *Phys. Rev. Lett.* **90**, 047002 (2003).
- [30] E. Gubankova, W. V. Liu, and F. Wilczek, Breached Pairing Superfluidity: Possible Realization in QCD, *Phys. Rev. Lett.* **91**, 032001 (2003).
- [31] A. Moreo, M. Daghofer, J. A. Riera, and E. Dagotto, Properties of a two-orbital model for oxypnictide superconductors: Magnetic order, B_{2g} spin-singlet pairing channel, and its nodal structure, *Phys. Rev. B* **79**, 134502 (2009).
- [32] A. Moreo, M. Daghofer, A. Nicholson, and E. Dagotto, Interband pairing in multiorbital systems, *Phys. Rev. B* **80**, 104507 (2009).
- [33] C. E. Matt, D. Sutter, A. M. Cook, Y. Sassa, M. Månsson, O. Tjernberg, L. Das, M. Horio, D. Destraz, C. G. Fatuzzo, K. Hauser, M. Shi, M. Kobayashi, V. N. Strocov, T. Schmitt, P. Dudin, M. Hoesch, S. Pyon, T. Takayama, H. Takagi *et al.*, Direct observation of orbital hybridisation in a cuprate superconductor, *Nat. Commun.* **9**, 972 (2018).
- [34] J. Tahir-Kheli, Interband pairing theory of superconductivity, *Phys. Rev. B* **58**, 12307 (1998).
- [35] O. V. Dolgov, E. P. Fetisov, and D. I. Khomskii, Superconductivity of heavy fermions in a two-band model, *Phys. Lett. A* **125**, 267 (1987).
- [36] E. Piatti, D. Romanin, and R. S. Gonnelli, Mapping multi-valley Lifshitz transitions induced by field-effect doping in strained MoS_2 nanolayers, *J. Phys.: Condens. Matter* **31**, 114002 (2019).
- [37] S. Poncé, E. R. Margine, C. Verdi, and F. Giustino, EPW: Electron-phonon coupling, transport and superconducting properties using maximally localized Wannier functions, *Comput. Phys. Commun.* **209**, 116 (2016).
- [38] J. Bekaert, L. Bignardi, A. Aperis, P. van Abswoude, C. Mattevi, S. Gorovikov, L. Petaccia, A. Goldoni, B. Partoens, P. M. Oppeneer, F. M. Peeters, M. V. Milošević, P. Rudolf, and C. Cepek, Free surfaces recast superconductivity in few-monolayer MgB_2 : Combined first-principles and ARPES demonstration, *Sci. Rep.* **7**, 14458 (2017).
- [39] H. Suhl, B. T. Matthias, and L. R. Walker, Bardeen-Cooper-Schrieffer Theory of Superconductivity in the Case of Overlapping Bands, *Phys. Rev. Lett.* **3**, 552 (1959).
- [40] F. G. Korchorbé and M. E. Palistrant, Superconductivity in a two-band system with low carrier density, *Zh. Eksp. Teor. Fiz.* **104**, 442 (1993).
- [41] F. Giubileo, F. Bobba, A. Scarfato, A. M. Cucolo, A. Kohen, D. Roditchev, N. D. Zhigadlo, and J. Karpinski, Local tunneling study of three-dimensional order parameter in the π band of Al-doped MgB_2 single crystals, *Phys. Rev. B* **76**, 024507 (2007).
- [42] F. Giubileo, D. Roditchev, W. Sacks, R. Lamy, D. X. Thanh, J. Klein, S. Miraglia, D. Fruchart, J. Marcus, and Ph. Monod, Two-Gap State Density in MgB_2 : A True Bulk Property or a Proximity Effect? *Phys. Rev. Lett.* **87**, 177008 (2001).
- [43] D. V. Efmremov, M. M. Korshunov, O. V. Dolgov, A. A. Golubov, and P. J. Hirschfeld, Time-reversal symmetry breaking state near the surface of an s_{\pm} superconductor, *Phys. Rev. B* **84**, 180512(R) (2011).
- [44] G. Ghigo, D. Torsello, G. A. Ummarino, L. Gozzelino, M. A. Tanatar, R. Prozorov, and P. C. Canfield, Disorder-Driven Transition from $s_{\pm}\hat{A}_{\pm}$ to s_{++} Superconducting Order Parameter in Proton Irradiated $\text{Ba}(\text{Fe}_{1-x}\text{Rh}_x)_2\text{As}_2$ Single Crystals, *Phys. Rev. Lett.* **121**, 107001 (2018).

- [45] A. Damascelli, Z. Hussain, and Z.-X. Shen, Angle-resolved photoemission studies of the cuprate superconductors, *Rev. Mod. Phys.* **75**, 473 (2003).
- [46] S. Souma, Y. Machida, T. Sato, T. Takahashi, H. Matsui, S.-C. Wang, H. Ding, A. Kaminski, J. C. Campuzano, S. Sasaki, and K. Kadowaki, The origin of multiple superconducting gaps in MgB_2 , *Nature (London)* **423**, 65 (2003).
- [47] S. A. Kuzmichev, T. E. Kuzmicheva, and S. N. Tchesnokov, Determination of the electron-phonon coupling constants from the experimental temperature dependences of superconducting gaps in MgB_2 , *JETP Lett.* **99**, 295 (2014).
- [48] H. J. Choi, D. Roundy, H. Sun, M. L. Cohen, and S. G. Louie, First-principles calculation of the superconducting transition in MgB_2 within the anisotropic Eliashberg formalism, *Phys. Rev. B* **66**, 020513(R) (2002).
- [49] A. Aperis, P. Maldonado, and P. M. Oppeneer, *Ab initio* theory of magnetic-field-induced odd-frequency two-band superconductivity in MgB_2 , *Phys. Rev. B* **92**, 054516 (2015).
- [50] I. I. Mazin, D. J. Singh, M. D. Johannes, and M. H. Du, Unconventional Superconductivity with a Sign Reversal in the Order Parameter of $\text{LaFeAsO}_{1-x}\text{F}_x$, *Phys. Rev. Lett.* **101**, 057003 (2008).
- [51] X. Lu, C. Fang, W.-F. Tsai, Y. Jiang, and J. Hu, *s*-wave superconductivity with orbital-dependent sign change in checkerboard models of iron-based superconductors, *Phys. Rev. B* **85**, 054505 (2012).
- [52] P. Zhang, P. Richard, T. Qian, X. Shi, J. Ma, L.-K. Zeng, X.-P. Wang, E. Rienks, C.-L. Zhang, P. Dai, Y.-Z. You, Z.-Y. Weng, X.-X. Wu, J. P. Hu, and H. Ding, Observation of Momentum-Confinement In-Gap Impurity State in $\text{Ba}_{0.6}\text{K}_{0.4}\text{Fe}_2\text{As}_2$: Evidence for Antiphase s_{\pm} Pairing, *Phys. Rev. X* **4**, 031001 (2014).
- [53] Z. P. Yin, K. Haule, and G. Kotliar, Spin dynamics and orbital-antiphase pairing symmetry in iron-based superconductors, *Nat. Phys.* **10**, 845 (2014).
- [54] H. Ding, K. Nakayama, P. Richard, S. Souma, T. Sato, T. Takahashi, M. Neupane, Y.-M. Xu, Z.-H. Pan, A. V. Fedorov, Z. Wang, X. Dai, Z. Fang, G. F. Chen, J. L. Luo, and N. L. Wang, Electronic structure of optimally doped pnictide $\text{Ba}_{0.6}\text{K}_{0.4}\text{Fe}_2\text{As}_2$: A comprehensive angle-resolved photoemission spectroscopy investigation, *J. Phys.: Condens. Matter* **23**, 135701 (2011).
- [55] N. W. Salovich, H. Kim, A. K. Ghosh, R. W. Giannetta, W. Kwok, U. Welp, B. Shen, S. Zhu, H.-H. Wen, M. A. Tanatar, and R. Prozorov, Effect of heavy-ion irradiation on superconductivity in $\text{Ba}_{0.6}\text{K}_{0.4}\text{Fe}_2\text{As}_2$, *Phys. Rev. B* **87**, 180502(R) (2013).
- [56] V. G. Stanev and A. E. Koshelev, Anomalous proximity effects at the interface of *s* and s_{\pm} superconductors, *Phys. Rev. B* **86**, 174515 (2012).
- [57] N. V. Orlova, A. A. Shanenko, M. V. Milošević, F. M. Peeters, A. V. Vagov, and V. M. Axt, Ginzburg-Landau theory for multiband superconductors: Microscopic derivation, *Phys. Rev. B* **87**, 134510 (2013).
- [58] J. W. Brendan and P. D. Mukunda, Time-reversal-symmetry-broken state in the BCS formalism for a multi-band superconductor, *J. Phys.: Condens. Matter* **25**, 425702 (2013).
- [59] J. Garaud, J. Carlström, and E. Babaev, Topological Solitons in Three-Band Superconductors with Broken Time Reversal Symmetry, *Phys. Rev. Lett.* **107**, 197001 (2011).
- [60] J. Garaud, J. Carlström, E. Babaev, and M. Speight, Chiral $\mathbb{C}P^2$ skyrmions in three-band superconductors, *Phys. Rev. B* **87**, 014507 (2013).
- [61] N. V. Orlova, P. Kuopanportti, and M. V. Milošević, Skyrmionic vortex lattices in coherently coupled three-component Bose-Einstein condensates, *Phys. Rev. A* **94**, 023617 (2016).
- [62] V. Stanev and A. E. Koshelev, Complex state induced by impurities in multiband superconductors, *Phys. Rev. B* **89**, 100505(R) (2014).
- [63] A. M. Bobkov and I. V. Bobkova, Time-reversal symmetry breaking state near the surface of an s_{\pm} superconductor, *Phys. Rev. B* **84**, 134527 (2011).
- [64] J. Garaud, M. Silaev, and E. Babaev, Change of the vortex core structure in two-band superconductors at the impurity-scattering-driven s_{\pm}/s_{++} crossover, *Phys. Rev. B* **96**, 140503(R) (2017).
- [65] D. Wang, L. Kong, P. Fan, H. Chen, S. Zhu, W. Liu, L. Cao, Y. Sun, S. Du, J. Schneeloch, R. Zhong, G. Gu, L. Fu, H. Ding, and H.-J. Gao, Evidence for Majorana bound states in an iron-based superconductor, *Science* **362**, 333 (2018).
- [66] J.-X. Yin, Z. Wu, J.-H. Wang, Z.-Y. Ye, J. Gong, X.-Y. Hou, L. Shan, A. Li, X.-J. Liang, X.-X. Wu, J. Li, C.-S. Ting, Z.-Q. Wang, J.-P. Hu, P.-H. Hor, H. Ding, and S. H. Pan, Observation of a robust zero-energy bound state in iron-based superconductor $\text{Fe}(\text{Te},\text{Se})$, *Nat. Phys.* **11**, 543 (2015).
- [67] R. S. Gonnelli, D. Daghero, G. A. Ummarino, A. Calzolari, M. Tortello, V. A. Stepanov, N. D. Zhigadlo, K. Rogacki, J. Karpinski, F. Bernardini, and S. Massidda, Effect of Magnetic Impurities in a Two-Band Superconductor: A Point-Contact Study of Mn-Substituted MgB_2 Single Crystals, *Phys. Rev. Lett.* **97**, 037001 (2006).
- [68] N. Kumar and K. P. Sinha, Possibility of photoinduced superconductivity, *Phys. Rev.* **174**, 482 (1968).
- [69] J. R. Abo-Shaer, D. E. Miller, J. K. Chin, K. Xu, T. Mukaiyama, and W. Ketterle, Coherent Molecular Optics Using Ultracold Sodium Dimers, *Phys. Rev. Lett.* **94**, 040405 (2005).
- [70] <http://www.multisuper.org>.